Special reprint
from
AEÜ ARCHIV FÜR ELEKTRONIK UND ÜBERTRAGUNGSTECHNIK
ELECTRONICS AND COMMUNICATION
Band 34 (1980), pp. 305–312

Investigation of Dark Current Shot Noise in CdS/CuInSe$_2$-Photodiodes with a Lock-in Technique

by Wolfgang Freude *

Report from the Institut für Hochfrequenztechnik und Quantenelektronik, Universität Karlsruhe

A very low noise measurement system is described with a noise temperature of 0.5 K consisting of a mercury wetted reed switch, low noise preamplifier, and synchronous detector. The set-up can te tuned from 20 kHz up to 3.15 GHz corresponding to the bandwidth of relay and preamplifier. The shot noise of CdS/CuInSe$_2$-photodiodes has been investigated. Deviations from the expected behaviour indicate avalanche effects, and the existence of a technologically entailed bypass resistance in parallel to the junction.

Untersuchung des Dunkelstromrauschens von CdS/CuInSe$_2$-Photodioden mit einem Lock-in-Verfahren

Ein sehr rauscharmes Meßsystem wird beschrieben. Es weist eine Rauschtemperatur von 0,5 K auf und besteht aus einem quecksilberbenetzten Reed-Schalter, einem rauscharmen Vorverstärker und einem Synchrondetektor. Die Anordnung kann entsprechend der Bandbreite von Schalter und Vorverstärker in einem Frequenzbereich von 20 kHz bis 3,15 GHz betrieben werden. Das Schrotrauschen von CdS/CuInSe$_2$-Photodioden wurde untersucht. Abweichungen vom erwarteten Verhalten deuten auf Lawineneffekte und auf das Vorhandensein eines technologisch bedingten Widerstandes parallel zur Sperrschicht.

1. Introduction

Photodetectors for the longer wavelength range above 1 μm are of growing importance, because dispersion and attenuation of optical glass-fibre waveguides near 1.3 μm and specially near 1.5 μm wavelength are lower than around 0.85 μm, where high-performance silicon detectors and GaAlAs emitters are available. Based on the quaternary alloy system InGaAsP opto-electronic devices for longer wavelengths were developed without having reached yet the technical standard of the 0.85 μm components.

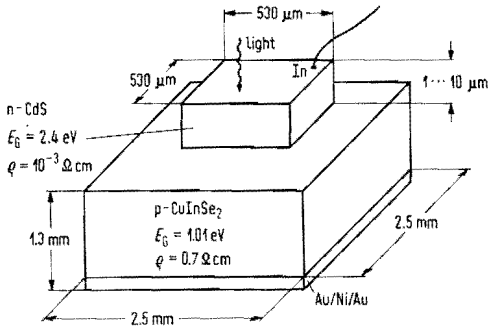

Fig. 1. Structure of CdS/CuInSe$_2$-photodetector.

An interesting alternative to the III–V alloys represents the I–III–VI$_2$ compound CuInSe$_2$ [1]–[3]. Fig. 1 shows a schematic of the investigated heterostructure photodiodes. On a single crystal p–CuInSe$_2$ substrate, grown by the Bridgeman-method with Se excess in the source material, a single crystal CdS layer has been deposited in a molecular-beam-epitaxy system forming mesa-type diodes by shadow-masking. During the process doping was accomplished by evaporation of In. Light with wavelengths beyond 0.51 μm striking the CdS-layer is not attenuated because of the high bandgap energy $E_G = 2.4$ eV, while the direct semiconductor CuInSe$_2$ with $E_G = 1.01$ eV absorbs the incident light on a very short distance [3], typically 2 μm. Assuming an abrupt junction, which is justified by the highly different doping levels in the CuInSe$_2$ and CdS layers, the depletion width can be determined by measuring the small-signal voltage dependent capacitance. With a reverse bias voltage of 4 V the junction is about 7 μm wide, so nearly all carriers can be generated in the drift region if the diffusion zones are kept small. This favours high quantum efficiency and fast response. For wavelengths of 0.55 μm up to 1.26 μm the quantum efficiency is greater than 60% with a flat top of 85% between 1.06 μm and 1.23 μm. The active area amounts to 0.3 mm^2. Current-voltage characteristics of the two investigated diodes are shown in Fig. 2. In contrast to former results [2], [3], these diodes exhibit a rather high dark current of about 50 μA at 4 V reverse bias, therefore a large dark current noise is to be expected. In a 50 Ω system the 3 dB bandwidth of these diodes with a zero bias capacitance 10 pF would be about 320 MHz, whereas for a diode with zero bias capacitance 22 pF a bandwidth of 70 MHz was measured [2] by a pulse-method, indicating an influence of carriers generated in the diffusion zones. This bandwidth is still large enough for the present 34 Mbit/s

* Dr. W. Freude, Institut für Hochfrequenztechnik und Quantenelektronik, Universität, Postfach 6380, D-7500 Karlsruhe 1.

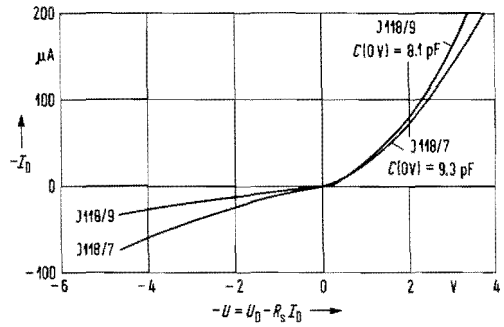

Fig. 2. Current-voltage characteristic of two CdS/CuInSe$_2$-photodiodes. C_j(0V) is the junction capacitance without bias.

systems, so the measured noise properties of the diode around 30 MHz are of main interest.

2. Experimental Set-up and Limiting Sensitivity

For this purpose a high-performance broad-band noise measurement system tunable from $f_0 =$ 20 kHz up to $f_0 = 3.15$ GHz was developed, Fig. 3. figuration with internal connection of one pole to the characteristic impedance $Z_L = R_C = 50\ \Omega$. Port A of the bias circuit is terminated with Z_L, too, $R_A = Z_L$. Both resistances are assumed to have the same temperature. The parallel resistance presented by R_S and the photodiode changes $R_{A\,input}$ by less than 0.5% if $R_j \| R_p \geqq 10\ k\Omega$. Because $C_j \leqq 10$ pF the influence of the junction capacitance is negligible up to frequencies of 30 MHz. For higher frequencies its presence must be considered. The switch is driven by a reference source with frequency $f_m = 5.4$ Hz and modulates the noise power seen by preamplifier[1] A_1. The single-sideband receiver[2] A_2 heterodynes part of the input spectrum of width B centered around f_0 down to an output spectrum centered around an IF f_B. The modulated output noise is linearly rectified and prefiltered by LR (Operational amplifier circuit). Lock-in amplifier[3] A_3 detects the periodic component f_m in the spectrum of the rectified output noise. The accuracy of the DC voltage reading U_{out} is determined by a built-in low-pass filter of bandwidth W. In contrast to correlation measurements with a Hanbury

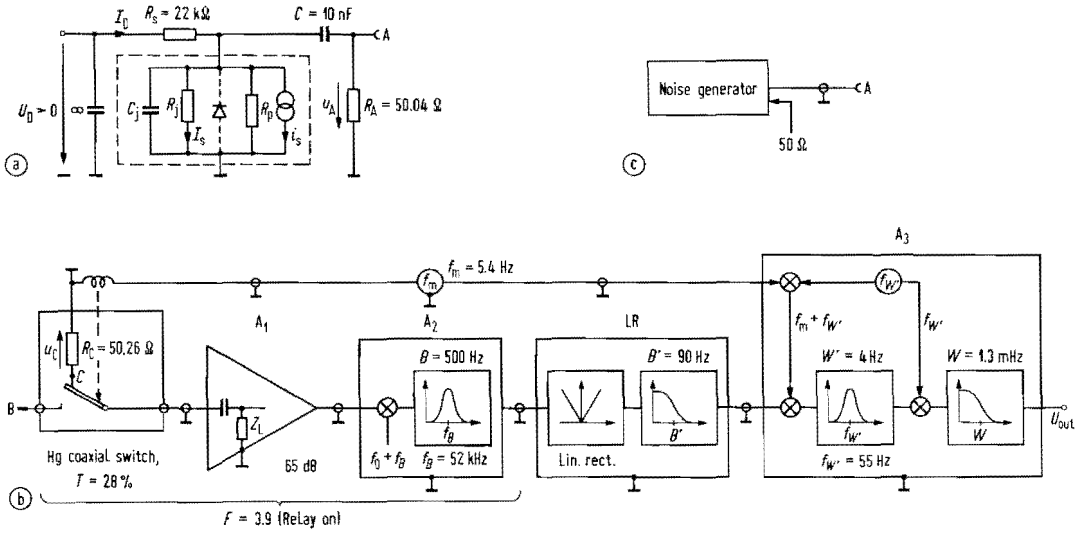

Fig. 3. Noise measurement equipment. All coaxial lines have a characteristic impedance of $Z_L = 50\ \Omega$.
(a) Bias circuit of photodiode, ——— marks the equivalent circuit of the diode.
(b) Noise synchronous detector, consisting of Hg coaxial switch driven by modulating source of frequency f_m, low-noise broadband (20 kHz to 3.15 GHz) preamplifier A_1, receiver A_2 with bandwidth B and IF-frequency f_B, linear rectifier LR with lowpass filter, synchronous detector A_3 with heterodyne front end of bandwidth W' and IF-frequency f_W, and demodulator with lowpass filter of bandwidth W.
(c) Noise generator for calibrating the set-up.

The light guarded photodiode with an equivalent circuit consisting of small-signal junction resistance R_j and junction capacitance C_j, a parasitic resistance R_p, and the shot noise current source $\overline{i_s^2} = 2eI_sB$ with the direct current I_S flowing through the junction, is biased by an extremely well filtered DC voltage U_D causing a current I_D flowing into the equivalent circuit of the photodiode. The noise power emitted at port A is coupled to input B of a mercury coaxial switch similar in construction to reference [4] but in a SPDT con- Brown-Twiss type circuit [6] the present set-up needs the costly amplifier chain only once and avoids the use of a broadband multiplier. Having finished the measurements with the apparatus of

[1] B & H Electronics AC-3020, 20 kHz — 3.15 GHz, 21 dB gain as first preamplifier. Avantek GPD-461, GPD-461, GPD-462 in cascade, 150 kHz — 700 MHz, 44 dB gain, or another B & H module as second preamplifier.

[2] Rohde & Schwarz, USVH, 10 kHz — 30 MHz, with additional IF-output.

[3] Ithaco, model 393 Dynatrac.

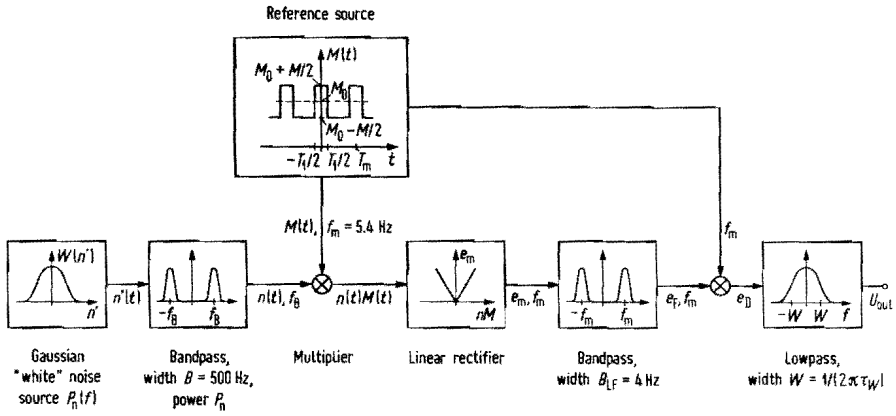

Fig. 4. Mathematical model of measurement system Fig. 3b.

Fig. 3 the author became aware of the close resemblance to the radiometer of Dicke [5]. The following theoretical treatment is based on Middleton [7] and Rowe [8]. It is believed to be more rigorous than that by Dicke [5], clarifying assumptions and simplifications.

The mathematical model of the measurement system is shown in Fig. 4. A noise source with Gaussian probability density $W(n')$ of the random voltage n' and zero mean value is filtered by a Gaussian narrowband filter of centerfrequency f_B and half-power bandwidth (HPBW) B yielding the random time function $n(t)$. Within the transmission range of the filter the noise source is assumed to be white having a Nyquist power spectrum $P(f) = 4kT_0Z_L$. A reference square-wave source $M(t) = M_0 + m(t)$ with period $T_m = 1/f_m$ and duty cycle $T = T_1/T_m$ modulates the bandpass-filtered noise voltage $n(t)$, where

$$m(t) = \sum_{q=-\infty}^{\infty} m_0(t + qT_m)$$

and

$$m_0(|t| < T_1/2) = M/2,$$
$$m_0(T_1/2 \leqq |t| < T_m/2) = -M/2,$$
$$m_0(|t| \geqq T_m/2) = 0.$$

$M_0 > |M/2|$ is assumed large enough so that no overmodulation will occur. As looked from the input port of the linear rectifier LR the systems Fig. 4, Fig. 3 behave identically, indeed, provided the probability density of the actual noise source does not deviate from a Gaussian density while switching the modulator from input port B to the internally connected termination resistance, and vice versa.

The rectifier detects the envelope of the modulated noise voltage $n(t)$, namely

$$e_m(t) = |n(t)M(t)|$$

or, since $M(t) > 0$ and $e(t) = |n(t)|$

$$e_m(t) = e(t)[M_0 + m(t)].$$

Because $M(t)$ and $n(t)$ are assumed to be statistically independent where $f_m \ll B$, the correlation function

$$R_x(\tau) = \overline{x(t)\,x(t-\tau)}$$

is written as

$$R_{e_m}(\tau) = M_0^2\left[1 + \frac{M}{M_0}(2T - 1)\right] \cdot \cdot R_e(\tau) + R_m(\tau)\,R_e(\tau). \tag{1}$$

Applying the Wiener-Khintchine theorem [7], [9] the two-sided power spectrum becomes

$$P_{e_m}(f) = M_0^2\left[1 + \frac{M}{M_0}(2T - 1)\right] \cdot \cdot P_e(f) + P_m(f) * P_e(f). \tag{2}$$

The asterisk denotes the convolution operator and $P_x(f)$ is the power spectrum of the random variable $x(t)$. Middleton [7] gives the low-frequency part $f \ll 2f_B$ of the second-moment function of a narrowband Gaussian process $n(t)$ after transformation by a linear full-wave rectifier as

$$R_e(\tau) = \frac{2P_n}{\pi}\,{}_2F_1[-\tfrac{1}{2}, -\tfrac{1}{2}; 1; r_{n0}^2(\tau)] = \frac{2P_n}{\pi}\sum_{l=0}^{\infty} a_l\, r_{n0}^{2l}(\tau), \quad a_l = \left[\frac{(-\tfrac{1}{2})_l}{l!}\right]^2, \tag{3}$$

$$a_0 = 1, \quad a_1 = 1/4, \quad a_2 = 1/64, \quad a_3 = 1/256, \quad a_4 = 1/655.36.$$

${}_2F_1$ is a hypergeometric function,

$$(z)_l = z(z+1)(z+2)\ldots(z+l-1)$$

Pochhammer's symbol, and $r_{n0}(\tau)$ stands for the envelope of the normalized correlation function $r_n(\tau) = R_n(\tau)/R_n(0)$ of the noise voltage $n(t)$ with the power spectrum

$$P_n(f) = \frac{P_n}{4\sqrt{\pi}\,W_B}\left\{\exp\left[-\frac{(f - f_B)^2}{4W_B^2}\right] + \exp\left[-\frac{(f + f_B)^2}{4W_B^2}\right]\right\}, \tag{4}$$

where $P_n = \overline{n^2(t)} = 4kT_0Z_LB$ equals the total noise power of $n(t)$ in a unit resistance, and the HPBW of the filter reads $B = W_B \cdot 4\sqrt{\ln 2} \approx 3.33\,W_B$. Applying the Wiener-Khintchine theorem to eq. (4) yields after normalization the correlation function

$$r_n(\tau) = r_{n0}(\tau)\cos\omega_0\tau\,,$$
$$r_{n0}(\tau) = \exp\left[-(2\pi W_B\tau)^2\right]. \tag{5}$$

From Fourier transforming eq. (3) the envelope power spectrum of $n(t)$ is obtained,

$$P_e(f) = \tag{6}$$
$$= \frac{2P_n}{\pi}\left[\delta(f) + \sum_{l=1}^{\infty} 2\sqrt{\frac{a_l}{2l\pi}}\,W_B \exp\left(-\frac{f^2}{8lW_B^2}\right)\right].$$

The power spectrum of the periodic modulation voltage $M(t)$ is calculated [9] to be

$$P_m(f) = \left(\frac{M}{2}\right)^2\left\{(2T-1)^2\delta(f) + \right. \tag{7}$$
$$\left. + \sum_{q=1}^{\infty} 4\left(\frac{\sin q\pi T}{q\pi}\right)^2\left[\delta(f-qf_m) + \delta(f+qf_m)\right]\right\}.$$

Substituting eqs. (6) and (7), eq. (2) becomes, having performed the convolution,

$$P_{em}(f) = \frac{2P_n}{\pi}\left\{M_0^2\left[1 + \frac{M/2}{M_0}(2T-1)\right]^2\delta(f) + \right.$$
$$+ M^2\sum_{q=1}^{\infty}\left(\frac{\sin q\pi T}{q\pi}\right)^2\left[\delta(f-qf_m) + \delta(f+qf_m)\right] +$$
$$+ M_0^2\left[1 + \frac{M/2}{M_0}(2T-1)\right]^2\sum_{l=1}^{\infty} 2\sqrt{\frac{a_l}{2l\pi}}\,W_B \cdot$$
$$\cdot\exp\left(-\frac{f^2}{8lW_B^2}\right) + \tag{8}$$
$$+ M^2\sum_{q=1}^{\infty}\sum_{l=1}^{\infty}\left(\frac{\sin q\pi T}{q\pi}\right)^2\frac{a_l}{2\sqrt{2l\pi}\,W_B}\cdot$$
$$\left.\cdot\left[\exp\left(-\frac{(f-qf_m)^2}{8lW_B^2}\right) + \exp\left(-\frac{(f+qf_m)^2}{8lW_B^2}\right)\right]\right\}.$$

Filtering by the narrow Gaussian bandpass filter with HPBW $B_{LF} = W_{LF}\cdot 4\sqrt{\ln 2}$ and transfer function

$$|H_{LF}(f)|^2 = \tag{9}$$
$$= \frac{1}{2}\left\{\exp\left[-\frac{(f-f_m)^2}{4W_{LF}^2}\right] + \exp\left[-\frac{(f+f_m)^2}{4W_{LF}^2}\right]\right\},$$

where $B_{LF} \ll B, f_m$, only frequency components around f_m are retained, and because $a_l \ll a_1$ for $l \geqq 2$, the sums in l are truncated after the first term, so the power spectrum $P_{eF}(f)$ of the filtered voltage $e_F(t)$ can be written approximately

$$P_{eF}(f) = P_{per}\tfrac{1}{2}\left[\delta(f-f_m) + \delta(f+f_m)\right] +$$
$$+ P_{cont}\frac{1}{2\sqrt{\pi}\,W_{LF}}|H_{LF}(f)|^2, \tag{10a}$$

$$P_{per} = \frac{2}{\pi}\left(\frac{\sin\pi T}{\pi}\right)^2 P_n M^2, \tag{10b}$$

$$P_{cont} = \frac{4a_1}{2\sqrt{2}}\frac{B_{LF}}{B}P_n M_0^2\left\{\left[1 + \frac{M/2}{M_0}(2T-1)\right]^2 + \right.$$
$$\left. + \left(\frac{M}{M_0}\right)^2(1-T)\,T\right\}. \tag{10c}$$

P_{per} and P_{cont} are the total bandpass output powers for the periodic and the continuous part of the spectrum in a unit resistance.

As a last stage the synchronous demodulator (homodyne receiver [10]) extracts the periodic part of the spectrum. Let this signal voltage be

$$s(t) = s_0\cos\omega_m t\,, \quad s_0 = \sqrt{2P_{per}}\,,$$

from eq. (10b), and the spectrum of the additive noise voltage $n_S(t)$

$$P_{n_s}(f) = P_{cont}|H_{LF}(f)|^2/(2\sqrt{\pi}\,W_{LF}) \tag{11}$$

with correlation function

$$R_{n_s}(\tau) = \int_{-\infty}^{\infty} P_{n_s}(f)\,e^{j2\pi f\tau}\,df.$$

The sum of signal $s(t)$ and noise $n_S(t)$ is multiplied by the phase-shifted reference voltage

$$s_\varphi(t) = s_{\varphi 0}\cos(\omega_m t + \varphi),$$

from which the correlation function

$$R_{e_D}(\tau) =$$
$$= \overline{[s(t) + n(t)]\,s_\varphi(t)\cdot[s(t-\tau) + n(t-\tau)]\,s_\varphi(t-\tau)} =$$
$$= R_{ss_\varphi}(\tau) + R_{s_\varphi}(\tau)\cdot R_{n_s}(\tau) \tag{12}$$

follows, because $\overline{n_S} = 0$ and the noise is assumed to be statistically independent from the signal. The power spectrum becomes with eq. (11) after performing the convolution

$$P_{e_D}(f) = \left(\frac{s_0 s_{\varphi 0}}{2}\right)^2\cos^2\varphi\,\delta(f) +$$
$$+ \frac{s_{\varphi 0}^2}{2}P_{cont}\exp\left(-\frac{f^2}{4W_{LF}^2}\right)\Big/(4\sqrt{\pi}\,W_{LF}) + \tag{13}$$
$$+ \left(\frac{s_0 s_{\varphi 0}}{2}\right)^2\tfrac{1}{2}\left[\delta(f-2f_m) + \delta(f+2f_m)\right].$$

$P_{e_D}(f)$ is filtered by the lowpass function

$$|H_{LP}(f)|^2 = \frac{1}{(\omega^2\tau_W^2+1)^2}\,, \quad W = \frac{1}{2\pi\tau_W}\,,$$
$$W \ll B_{NF}, 2f_m\,,$$

which yields the spectrum $P_{out}(f)$ of the output voltage U_{out},

$$P_{out}(f) = P_{DC}(f) + P_{RMS}(f)\,,$$
$$P_{DC}(f) = \frac{s_{\varphi 0}^2}{2}P_{per}\cos^2\varphi\,\delta(f)\,, \tag{14}$$
$$P_{RMS}(f) = \frac{s_{\varphi 0}^2}{2}\frac{P_{cont}}{4\sqrt{\pi}\,W_{LF}}\frac{1}{(\omega^2\tau_W^2+1)^2}\,.$$

Applying Parseval's theorem gives the total power in a unit resistance for the DC and the fluctuating part of the output voltage,

$$U_{out} = U_{DC} + U_{RMS}\,,$$
$$U_{DC} = \sqrt{\int_{-\infty}^{\infty} P_{DC}(f)\,df} = \frac{s_{\varphi 0}}{\sqrt{\pi}}\frac{\sin\pi T}{\pi}\cos\varphi\sqrt{P_n}M\,,$$
$$U_{RMS} = \sqrt{\int_{-\infty}^{\infty} P_{RMS}(f)\,df} = \frac{s_{\varphi 0}}{2}\left(\frac{\pi\ln 2}{8}\right)^{1/4}\cdot \tag{15}$$
$$\cdot\sqrt{P_n}\sqrt{\frac{W}{B}}\,M_0\left\{\left[1 + \frac{M/2}{M_0}(2T-1)\right]^2 + \right.$$
$$\left. + \left(\frac{M}{M_0}\right)^2(1-T)\,T\right\}.$$

To state eq. (15) in words, the DC output voltage U_{DC} of the synchronous detector A_3 in Fig. 3 is proportional to the difference $\sqrt{P_n}M$ of the RMS noise voltage at input port B of the coaxial switch and the RMS noise voltage from the reference resistance R_C. The fluctuating part U_{RMS} of U_{out}, which limits the accuracy of the reading, is proportional to the square root of the mean noise power at the input of LR times the ratio of lowpass and HF bandwidth times M_0^2. With the switch at rest $M=0$, there are only fluctuations at the output port of A_3 from the thermal noise P_n of R_C and from the noise of amplifiers A_1, A_3. This total noise power is named $P_n M_0^2$ in eq. (15), so one can identify M_0^2 with the noise figure F of the amplifier chain. The lower the spectral density of the source resistance noise $P_n/B = 4kT_0Z_L$, the lower the lowpass bandwidth W, and the lower the noise figure F of the receiver, the less fluctuations are observed in U_{out}. On the other hand, the larger the total input noise power $P_n = 4kT_0Z_LB$, i.e. the larger the HF bandwidth, the higher a DC output voltage will be measured for a given difference M in the relative noise voltages from port B and C of the switch.

The relative accuracy of the output reading, denoted as noise-to-signal ratio for voltages $NSR_U = U_{RMS}/U_{DC}$, becomes from eq. (15) for $M \ll M_0$ and $\cos\varphi = 1$

$$NSR_U = \frac{[(\pi^7/8)\ln 2]^{1/4}}{2\sin\pi T}\sqrt{\frac{W}{B}}\,\frac{M_0}{M} \tag{16}$$

with a limiting value M_c for $NSR_U = 1$ of

$$M_c = \frac{[(\pi^7/8)\ln 2]^{1/4}}{2\sin\pi T}\sqrt{\frac{W}{B}}\,M_0 \approx 2.01\sqrt{\frac{W}{B}}\,M_0, \tag{17}$$

where the approximation is valid for a duty cycle $T \approx 50\%$. Eq. (16) expresses the fact that when amplitude modulating an incoherent narrowband noise carrier a low NSR can be obtained only if the carrier bandwidth B is much greater than the effective (de)modulation bandwidth W in consistence with the results of Rowe [8] and Grau [11].

While modulating, the noise level at the LR input is P_nF during $T_1/2 \leqq |t| < T_m/2$ and P_nF_{obj} during $|t| < T_1/2$, changed from the former value by the influence of the measured object at port A of the switch. Therefore

$$\begin{aligned} F_{obj} &= (M_0 + M/2)^2, \qquad F = (M_0 - M/2)^2, \\ M_0 &= \tfrac{1}{2}(\sqrt{F_{obj}} + \sqrt{F}), \quad M = \sqrt{F_{obj}} - \sqrt{F}. \end{aligned} \tag{18}$$

With eqs. (17) and (18) for $M \ll M_0$ the minimum detectable equivalent temperature difference $\Delta T = T_{obj} - T_C$ between object temperature $T_{obj} \gtrless T_A$, T_A as temperature of resistance R_A, and the reference temperature $T_C = T_0$ of resistance R_C becomes

$$\Delta T_c = FT_0\,2\,M_c/M_0 \approx FT_0 \cdot 2 \cdot 2.01\sqrt{W/B}. \tag{19}$$

This result corresponds to eq. (22) of Dicke [5], if a Gaussian gain profile of his wideband amplifier, and single-sideband conversion is assumed.

For calibration purposes a standard noise source with Gaussian statistics and generator resistance Z_L at reference temperature T_0 can be connected to port B of the switch while recording the voltage U_{DC} at the output of A_3 at different frequencies. From eqs. (15), (18) and Fig. 3 one gets

$$U_{DC} = G\left(\sqrt{\overline{u_A^2}} - \sqrt{\overline{u_B^2}}\right) = G\sqrt{\overline{\Delta u^2}},$$

where $\sqrt{\overline{\Delta u^2}}$ is the excess noise RMS voltage delivered from the calibration standard at port B. Because $\sqrt{\overline{\Delta u^2}}$ is known the gain G can be determined. Generally spoken $G = G(f)$ will be frequency dependent owing to the frequency dependence $F = F(f)$ of the receiver noise figure.

3. Experimental Results

Noise measurements were performed using the calibrated set-up of Fig. 3. Two CdS/CuInSe$_2$-diodes, serial number J 118/7 and J 118/9, were operated with a reverse bias current ranging from zero up to 300 μA maximum. With diode J 118/9 a certain DC instability could be observed for currents above 30 μA. In Fig. 5 the ratio of the measured shot noise equivalent current $I_s = \overline{i_s^2}/(2eB)$, Fig. 3a, and the current I_D into the device is plotted for frequencies from 1 MHz up to 30 MHz with the device current I_D as parameter. Shown as a broken horizontal line is the direct current equivalent of the minimum detectable mean square value of the noise current i_s in Fig. 3a,

$$\overline{i_{sc}^2} = 2e\,I_{sc}\,B = 4k\Delta T_c\,B/Z_L,$$

therefore (20)

$$I_{sc} = \frac{2k}{e}\frac{\Delta T_c}{Z_L} \approx 3.45\,\frac{\mu A}{K}\cdot 2 \cdot 2.01\,FT_0\sqrt{\frac{W}{B}},$$

which is normalized in Fig. 5 to the device current $I_D = 10$ μA. As can be seen the measured noise is partly far above and partly far below the theoretically expected level $I_s/I_D = 1$. With $I_s/I_D < 1$ this can be explained by a parasitic resistance R_p, Fig. 3a. Nonideal masking during forming the n-layer in Fig. 1 could have caused a surface current path, but the detailed nature of R_p is unknown. As a consequence the junction current is diminished, so with the externally measured differential diode resistance $R = R_j \| R_p \approx U_D/I_D - R_s$ the parasitic resistance R_p and the junction resistance R_j are calculated to be $R_p = R/(1 - I_s/I_D)$ and $R_j = RI_D/I_s$, which yields $R_j \approx 375$ kΩ, $R_p \approx 250$ kΩ for diode J 118/9 with $I_D = 30$ μA, $I_s/I_D \approx 0.4$, $R \approx 150$ kΩ and $R_j \approx 280$ kΩ, $R_p \approx 90$ kΩ for diode J 118/7 with $I_D = 30$ μA, $I_s/I_D \approx 0.25$, $R = 70$ kΩ. For $I_s/I_D > 1$ the deviations from undisturbed shot noise are probably caused by avalanche multiplication in the junction. At first sight the measured power spectrum seems to exhibit characteristics similar to $1/f$-noise, but from experiments with silicon bipolar transistors [12] follows, that $1/f$-noise cannot be observed at frequencies higher than about 100 kHz. If it is allowed to transfer this

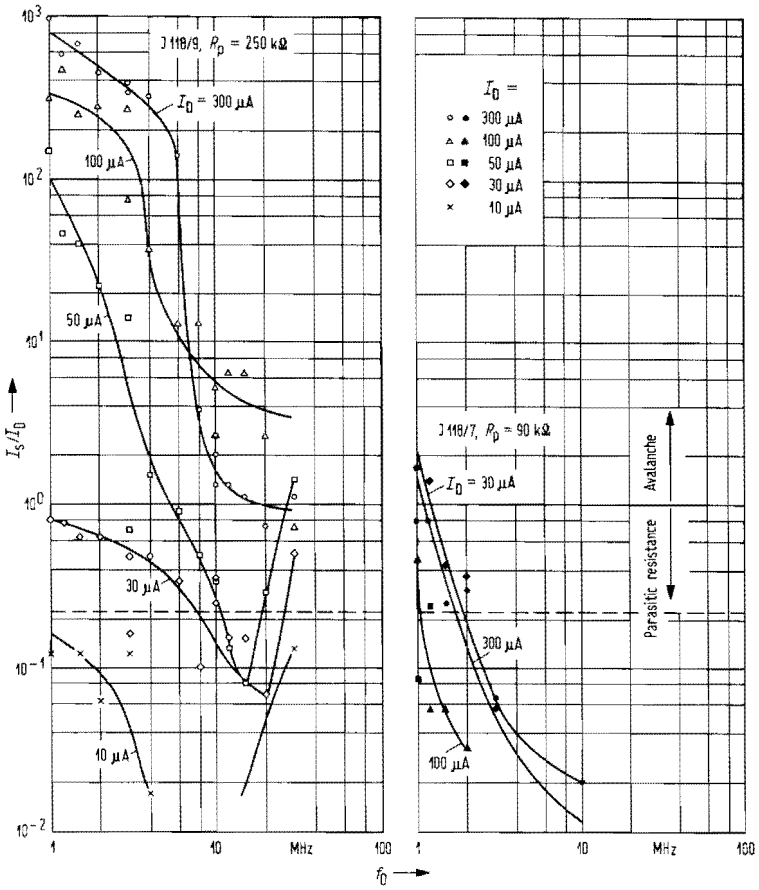

Fig. 5. Noise measurement results: Ratio of the measured shot noise equivalent current $I_s = \overline{i_s^2}/(2eB)$ and the direct current I_D into the photodiode in dependence of frequency with I_D as parameter. The broken line indicates the limiting sensitivity for I_s normalized to $I_D = 10$ µA.

result to the I–III–VI_2 compound under discussion, as a next guess the avalanche effect is made responsible for the observed deviation. To support this hypothesis the following procedure was adopted for the diode J 118/9, where the effect is more pronounced because of the higher resistance R_p: With known $I_D(U)$-characteristic, Fig. 2, the junction characteristic $I_d(U) \approx I_D(U) - U/R_p$ and the avalanche multiplication factor $M_{av} = I_d(U)/I_d(4\,V)$ can be calculated. The avalanche noise power P_{av} is given by [13]

$$P_{av}(M_{av}) \sim 2eI_d(M_{av}=1)\,BM_{av}^2 F_{exc}(M_{av}) \cdot \cdot [1 + (\omega M_{av}\tau_1)^2]^{-1} \sim I_s(M_{av}), \qquad (21)$$

(for a recent treatment of avalanche noise see [14], [15]), where $F_{exc}(M_{av}) \approx \text{const} \cdot M_{av}^x$ is called excess noise factor and τ_1 the intrinsic response time of the avalanche. The measured ratio

$$I_s(M_{av})/I_s(M_{av}=1) = M_{av}^2 M_{av}^x$$

for a fixed frequency near 1 MHz with $\omega \ll \omega_c = 1/(M_{av}\tau_1)$ can be fitted to yield the parameter x. Averaging $I_s(M_{av})$ from Fig. 5 over the frequency range 1 to 2 MHz, $\bar{I}_s(M_{av})$ was determined resulting in $x = 0.8$. This number does not contradict the theoretically expected value $0 \leq x \leq 1$ for avalanche noise. Following reference [12], a current dependence $I_s \sim I_d^y$ with $1 \leq y \leq 2$ should be observed for $1/f$-noise in junction diodes which was not true $(y = 2 + x)$ with the present experiment. Nevertheless the frequency dependence of the measured noise cannot be explained by the low-pass factor in eq. (21), because with reduced M_{av} the limiting frequency ω_c should increase, which was not observed. Whether the small-signal characteristic of the diode is responsible for this phenomenon, or whether there exists another superimposed effect (as burst noise), has not been further investigated.

Microplasma formation could be responsible for the observed instabilities in the external direct current I_D. The avalanche effect makes the choice of the "right" ratio I_s/I_D somewhat arbitrary for determining R_p, which is perhaps voltage dependent. Therefore the given figures should be regarded as order of magnitudes only. In any case this measurement gives a deeper insight into the diode properties, because characteristics of the junction alone can be studied. Needless to say that $I_s/I_D = 1$ does not prove any ideal shot noise behaviour of the junction.

These results show that the measured high dark currents do not detoriate the noise performance of the photodiodes significantly, if the yare embedded in a low-impedance environment.

4. Error Sources and Practical Limiting Sensitivity

Several sources of error were involved in the experiments.

a) First of all the noise figure $F = 3.9$ of the amplifier cascade A_1, A_2 and the bandwidth ratio W/B with $W = 1.3$ mHz, $B = 500$ Hz determine the lowest detectable power. From eqs. (19), (20) at $T_0 = 290$ K $\Delta T_c \approx 7$ K, $I_{sc} \approx 24$ µA for a duty cycle $T = 50\%$ is to be expected, therefore the effective lowpass bandwidth W_{eff} was reduced by averaging up to $n = 120$ samples U_{DC} so that $W_{eff} = W/n \approx 11$ µHz, resulting in $\Delta T_c \approx 0.6$ K, $I_{sc} \approx 2$ µA for a duty cycle $T = 28\%$. The minimum detectable spectral power density $k\Delta T_c \approx 8 \cdot 10^{-24}$ W/Hz compares favourably with the measured variance of the indication without any photodiode but with the bias source U_D connected, or with $I_D = 0$, namely $\Delta T_{c\,meas} = 0.5$ K, $k\Delta T_{c\,meas} = 6.4 \cdot 10^{-24}$ W/Hz, $I_{sc\,meas} = 1.6$ µA. Because TEM lines are coupled to the noise source only one

mode of the equivalent temperature radiation is detected, therefore the limiting number of photons becomes

$$S_c = \{\exp[hf_0/(k\Delta T_c)] - 1\}^{-1}$$

where f_0 stands for the center frequency to which the receiver is tuned. Evaluation yields

$$S_c(f_0 = 30\,\text{MHz}) = 400\,, \quad S_c(f_0 = 2.46\,\text{GHz}) = 4.4\,,$$

which can be well compared to the limiting sensitivity of a noise set-up with a maser [16] at center frequency $f_0 = 2.46$ GHz where $\Delta T_{c\,meas} = 1.6$ K, $k\Delta T_{c\,meas} = 2.2 \cdot 10^{-23}$ W/Hz, $S_c = 13$ could be measured.

In determining the intrinsic response time of silicon avalanche photodiodes (APD) and their excess noise the slightly modified set-up of Fig. 3 has been successfully used [17] at a frequency $f_0 = 2.7$ GHz, where HeNe laser light incident on a biased APD was switched by a chopper wheel with $f_m = 1$ kHz. Here the sensitivity could be improved by a factor 2 because a double-sideband receiver was available. With a receiver bandwidth $B = 2$ MHz the lowpass bandwidth was increased to $W = 16$ mHz, so with $F = 25$ $\Delta T_c = FT_0 \cdot 2.01\sqrt{W/B} = 1.3$ K, $k\Delta T_c = 1.8 \cdot 10^{-23}$ W/Hz, $I_{sc} = 4.5$ μA. The measurement showed a limiting sensitivity $I_{sc\,meas} = 1.5$ μA for a multiplication factor of $M_{av} = 4.75$. Because an excess noise factor of $M_{av}^{0.8}$ the shot noise power is increased to

$$k\Delta T_{c\,meas} = i_{sc\,meas}^2 M_{av}^{0.8} Z_L/(4B) = \\ = \tfrac{1}{2} e\, I_{sc\,meas} M_{av}^{0.8} Z_L = 2 \cdot 10^{-23}\,\text{W/Hz}$$

with an error of about 20% in agreement with the theoretical considerations above.

If in Fig. 3 for center frequencies $f_0 > 50$ MHz a rectifier usable at higher IF frequencies f_B would be employed the HF bandwidth could be widely enlarged to $B \approx 10$ MHz. Because the noise figure of the preamplifier A_1 changes only by 10% from $f_0 = 20$ kHz up to $f_0 = 3.15$ GHz, a limiting sensivity of $\Delta T_c = 0.05$ K, $k\Delta T_c = 7 \cdot 10^{-25}$ W/Hz, $I_{sc} = 170$ nA, $S_c(f_0 = 700\,\text{MHz}) = 1$ for $W = 1.3$ mHz, or, with numerically averaging over $n = 120$ samples $\Delta T_c = 0.005$ K, $k\Delta T_c = 6 \cdot 10^{-26}$ W/Hz, $I_{sc} = 16$ nA, $S_c(f_0 = 60\,\text{MHz}) = 1$ could be achieved theoretically. Considering the uncertainty principle the absolute minimum noise temperature $\Delta T_{c\,abs} = hf_0/(k \ln 2)$ of a linear amplifier which adds Gaussian noise to the signal is reached for an average number of $S_{c\,abs} = 1$ photon detected during the observation time $(2\pi W)^{-1}$ and $(2\pi W_{eff})^{-1}$, respectively [18].

b) On this point a second source of error has to be considered, namely possible temperature differences between R_A and R_C. A small offset into the negative range was observed for U_{DC}, indeed, indicating $T_C > T_A$ with the photodiode disconnected, because R_C was located nearer to the driving (and heating) coil of the reed switch than R_A. This offset as measured by a thermometer was about $\Delta T_0 = T_A - T_C = -2$ K with an error of 30% and could be compensated by a complementary offset in resistances R_C and R_A as described in c). A similar technique was used by Garrison and Lawson in constructing an absolute noise thermometer [19], [20].

c) A dominant error source in practical systems constitute the differences in source resistance as seen from ports B and C of the switch. For simplicity only the difference $\Delta R = R_C - R_A$ of the real impedances near the reference port and the measurement object is regarded. Because of the AC input coupling of amplifier A_1 no DC component will flow out of A_1 into R_A, R_B, R_C, therefore differences in additional shot noise are of no influence. Most important are the differences in noise figure and in the available noise power at the output of A_1. As an example the noise figures of A_1 at $f_0 = 8$ MHz for $R'_A = 50\,\Omega$, $R''_A = 60\,\Omega$ were measured to be $F' = 3.87$, $F'' = 3.57$ with an accuracy of about 3%. The noise power at the output port of A_1 amounts to $P_n = kFT_0B\Gamma$, where $\Gamma \sim R_A^{-1}(1/Z_L + 1/R_A)^{-2}$ is the source dependent gain of A_1 with input resistance Z_L and neglected feedback. Therefore the output noise powers can be written

$$P'_n = 4kF'T_0B\Gamma'\,, \\ P''_n = P'_nF''/F'R'_A(1/Z_L + 1/R'_A)^2 \cdot \\ \cdot R''^{-1}_A(1/Z_L + 1/R''_A)^{-2}\,.$$

A linear interpolation yields

$$\Delta = \frac{\Delta P_n(R'_A)}{P'_n} = b\,\frac{\Delta R_A}{R_A}\,,$$

with $\Delta = (P''_n - P'_n)/P'_n = -8.5 \cdot 10^{-2}$, $\Delta R_A = R''_A - R'_A = 10\,\Omega$, $b = -0.4$. From eq. (18) the effective modulation height becomes

$$M_{eff} = \sqrt{F_{obj} - \sqrt{F} = \sqrt{F'}(1 + \Delta) - \sqrt{F'} \approx \sqrt{F'}\,\Delta/2,} \\ M_{0\,eff} \approx \sqrt{F'}\,.$$

M_c in eq. (19) is to be replaced by M_{eff} leading to an impedance mismatch limiting sensivity of

$$\Delta T_{eff} = FT_0\Delta = bFT_0\Delta R_A/R_A. \qquad (22)$$

$\Delta R_A/R_A = (R_A - R_C)/R_A = -0.44\%$, so one estimates $\Delta T_{eff} = +2$ K with an error of about 70%. This positive effective temperature offset partly compensates for the genuine temperature offset, section 4b, in agreement with a measured offset $\Delta T_{c\,meas} = -0.3$ K. The influence of R_s has been neglected.

For using the ultimate sensitivity $\Delta T_c = 0.005$ K the source resistance should differ by not more than about 10^{-5}, which seems to be not very feasible in the microwave range. Therefore the practical limit will be specified by eq. (22) rather than by eq. (19), if not some sort of compensation scheme between temperature difference and resistance offset is implemented. With the preamplifier A_1 operated near its absolute noise figure minimum while maintaining input impedance matching, the influence of ΔR_A will be greatly reduced.

d) A further source of error, switching spikes by bouncing, by differing contact voltages in either position of the switch, and by pick-up of power line hum can be kept small using mercury wetted contacts and a modulating frequency $f_m \ll f_0$ together with appropriate low-frequency prefiltering.

e) The linearity of the system has been tested up to excess noise temperatures of $\Delta T = 13$ K and proved to be excellent.

f) Long-term stability of the amplifiers A_1, A_2 was obtained by line powering with a regulated supply.

g) Last not least it should be reminded that the statistic of the noise source investigated must not deviate from a normal distribution. From the central limit theorem [7] it follows directly, that the shot noise current i_s, albeit originally Poisson distributed, belongs to a normal process regardeless of the parameters of the individual shot noise pulses, provided that in the external circuit only the sum of many individual pulses can be observed. With a photodiode junction of 7 µm width and assumed drift velocities of about $5 \cdot 10^4$ m/s a single current impulse lasts less than 140 ps. If the sum of at least 10 individual impulses acts on the observing instrument, a rate of at least 1/14 ps = $70 \cdot 10^9$/s impulses is requested leading to a minimum direct current of about 10 nA. Then the hypothesis of Gaussian noise will hold. With minimum limiting currents of $I_{sc} = 1.6$ µA this condition is fulfilled, and even with the large bandwidth system and a theoretical limit of $I_{sc} = 16$ nA not violated. The bandpass characteristic of amplifiers A_1, A_2 further reduces the minimum allowable current.

5. Conclusion

A very low noise measurement systems has been demonstrated which is capable to detect excess noise temperatures of $\Delta T_c = 0.5$ K with a tuning range from 20 kHz up to 3.15 GHz, corresponding to a minimum detectable power of $k\Delta T_c = 6.4 \cdot 10^{-24}$ W/Hz or a minimum shot noise equivalent direct current of $I_{sc} = 1.6$ µA. An improvement by one order of magnitude seems to be feasible if the HF bandwidth for the higher frequency range is increased from 500 Hz to 10 MHz.

With this set-up CdS/$CuInSe_2$-photodiodes were investigated. Deviations from the expected shot noise powers indicate avalanche breakdown and a parasitic resistance in parallel to the junction.

Acknowledgements

The author would like to thank Dr. K. Hess, Dr. K. Lösch and Dr. R. Dorn from Standard Elektrik Lorenz, Stuttgart, for supplying the photodiodes and for discussions, and Prof. Dr. techn. G. K. Grau, University of Karlsruhe, for refering to the paper of Rowe [8].

(Received February 4th, 1980.)

References

[1] Haupt, H., Herstellung von Einkristallen und kristallinen Schichten für Bauelemente der optischen Nachrichtentechnik. Unpublished work.

[2] Dorn, R. et al., Efficient photovoltaic CdS/$CuInSe_2$ detectors for wavelength above 1 µm. Paper orally presented at ESSDERC 1978, Montpellier, France.

[3] Hess, K., Cds/$CuInSe_2$-Fotodektoren für optische Nachrichtenübertragung bei 1200 nm. Nachrichten Elektronik Heft 6 [1979], 185–186.

[4] Freude, W., Inexpensive equipment for driving GaAs lasers with 100 ps risetime pulses. Electron. Letters **12** [1976], 598–599.

[5] Dicke, R. H., The measurement of thermal radiation at microwave frequencies. Rev. Sci. Instrum. **17** [1946], 268–275.

[6] Chen, T.-M. and van der Ziel, A., Hanbury Brown-Twiss type circuit for measuring small noise signals. Proc. IEEE **53** [1965], 395.

[7] Middleton, D., An introduction to statistical communication theory. McGraw-Hill Book Co., New York 1960.

[8] Rowe, H. E., Amplitude modulation with a noise carrier. Proc. IEEE **52** [1964], 389–395.

[9] Papoulis, A., Probability, random variables and stochastic processes. McGraw-Hill Book Co., New York 1965.

[10] Grau, G. K., Quantenelektronik. Vieweg-Verlag, Braunschweig 1978.

[11] Grau, G. K., Rauschen im optischen Spektralbereich. Z. angew. Phys. **17** [1964], 21–26.

[12] Wolf, D., 1/*f*-noise. Noise in physical systems: Proc. Fifth Conf. on Noise, Bad Nauheim, Fed. Rep. of Germany, March 13–16, 1978. Springer-Verlag, Berlin 1978.

[13] Kaneda, T. and Takanashi, H., Avalanche buildup time of silicon avalanche photodiodes. Appl. Phys. Letters **26** [1975], 642–644.

[14] Van Vliet, K. M. and Rucker, L. M., Theory of carrier multiplication and noise in avalanche devices — Part I: One-carrier. IEEE Trans. ED-**26** [1979], 746–751.

[15] Van Vliet, K. M., Friedmann, A., and Rucker, L. M., Theory of carrier multiplication and noise in avalanche devices — Part II: Two-carrier. IEEE Trans. **ED-26** [1979], 752–764.

[16] Schneider, G., Measurement of the thermal noise of a superconducting resonator. AEÜ **25** [1971], 202–204.

[17] Freude, W., Performance of packaged fast silicon photodetectors in a broadband coaxial mount. AEÜ **31** [1977], 167–170. Erratum AEÜ **32** [1978], 43.

[18] Heffner, H., The fundamental noise limit of linear amplifiers. Proc. IRE **50** [1962], 1604–1608.

[19] Garrison, J. B. and Lawson, A. W., An absolute noise thermometer for high temperatures and high pressures. Rev. Sci. Instrum. **20** [1949], 785–794.

[20] Storm, L., Noise thermometry with conventional electronis. Noise in physical systems: Proc. Fifth Conf. on Noise, Bad Nauheim, Fed. Rep. of Germany, March 13–16, 1978. Springer-Verlag, Berlin 1978.